PROCEEDINGS OF SPIE

SPIEDigitalLibrary.org/conference-proceedings-of-spie

Protein-based molecular contrast optical coherence tomography

Changhuei Yang, Michael A. Choma, Laura E. Lamb, John D. Simon, Joseph A. Izatt

Changhuei Yang, Michael A. Choma, Laura E. Lamb, John D. Simon, Joseph A. Izatt, "Protein-based molecular contrast optical coherence tomography," Proc. SPIE 5316, Coherence Domain Optical Methods and Optical Coherence Tomography in Biomedicine VIII, (1 July 2004); doi: 10.1117/12.531353

SPIE.

Event: Biomedical Optics 2004, 2004, San Jose, CA, United States

Protein Based Molecular Contrast Optical Coherence Tomography

Changhuei Yang[a], Michael A. Choma[a], Laura E. Lamb[b], John D. Simon[b], Joseph A. Izatt[a]

[a]Biomedical Engineering Department, 136 Hudson Hall, Duke University, Durham NC 27708
[b]Chemistry Department, 101 Gross Chemistry Laboratory, Duke University, Durham NC 27708

ABSTRACT

We describe a novel technique for contrast enhancement in optical coherence tomography (OCT) which uses optically switchable protein based chromophores. Photosensitive proteins, such as bacteriorhodopsin and phytochrome, are promising OCT molecular contrast agents by reason of their remarkably low transition activation intensities compatible with *in vivo* imaging, and their potential for use as genetically expressible markers for molecular imaging. This study details the use of a novel optical switch suppression scheme which uses the absorption change between the two state groups of phytochrome to extract concentration and distribution information of the contrast agent within a target sample.

Keywords: molecular contrast, optical coherence tomography. protein, phytochrome

1. INTRODUCTION

Optical coherence tomography (OCT) is an emerging tool for real time in-situ tissue imaging with micrometer-scale resolution to depths of a few mm in highly scattering media. Real-time OCT systems have been integrated into clinical medical diagnostic instruments, and functional extensions such as polarization-sensitive, Doppler, and spectroscopic OCT have recently been introduced. These functional enhancements add the ability to discern contrast due to fibrous structure and orientation, motion, and to some extent absorber concentration in samples such as biological tissues. However, OCT remains a relatively contrast-starved imaging modality due to the low contrast in scattering coefficient between biological tissue types. In comparison, fluorescence contrast microscopy [1] (including single and multi-photon variants) has had tremendous impact in biology and medicine because of its capability to image highly specific molecular targets, including antibody-conjugated fluorescent probes and genetically expressible probes such as fluorescent proteins. However, the penetration depth of fluorescence microscopy is limited, and the potential for *in vivo* use of exogenous fluorophores is limited due to their toxicity and by singlet oxygen formation within the sample. Recent OCT research development has begun to look into methods that can begin to provide contrast (chemical [2]or otherwise [3]) capability to OCT. This class of OCT schemes, which we shall classify as molecular contrast OCT (MCOCT), combines the major advantages of fluorescence microscopy and OCT – contrast agent specificity of the former and, the higher spatial resolution and depth penetration of the later. A highly desirable addition capability that such imaging systems can have is the capability to detect protein based contrast agents. The rapid and widespread adaptation of green fluorescence protein (GFP) based fluorescence microscopy technique [4] for biology research points to the usefulness of protein based contrast agent based imaging modalities, especially if the contrast agent in question is endogenous and amendable to genetic manipulation for targeted gene expression.

In this report, we present a novel molecular contrast OCT (MCOCT) technique for detection of protein based contrast agents within a target sample. As with our previous work [2], our strategy is centered on the use of molecular contrast agents which can be modulated between states with differing absorption spectra at the OCT wavelength by the application of an external field, for example a pump laser pulse. Depending upon the lifetime of the probed states and the speed of the OCT system, the contrast agent molecules are probed by a pair of subsequently acquired OCT pixels, A-scans, or images, and the location and the concentration of the agents within the target sample is deduced from the resulting spatially localized differential signal. To extend this technique to protein-based chromophores, we report on the use of a class of bistable biochemical optical switches, such as phytochrome and bacteriorhodopsin. In response to illumination at the appropriate wavelength, these switches exhibit a reversible conformational change to a different

Coherence Domain Optical Methods and Optical Coherence Tomography in Biomedicine VIII, edited by Valery V. Tuchin, Joseph A. Izatt, James G. Fujimoto, Proc. of SPIE Vol. 5316 (SPIE, Bellingham, WA, 2004) · 1605-7422/04/$15 · doi: 10.1117/12.531353

absorptive state (Fig. 1). The use of these chromophores as contrast agents has several major advantages for MCOCT: 1) since the effective lifetime of both bistable states is under experimental control, remarkably low transition activation intensities compatible with *in vivo* imaging can be achieved, 2) protein-based chromophores are genetically expressed under promoter control, and thus have the potential for use as transfected genetic markers, 3) the use of absorptive rather than fluorescent protein chromophores for contrast avoids singlet oxygen generation, increasing the potential for *in vivo* use.

2. CONTRAST AGENT CHOICE: PHYTOCHROME

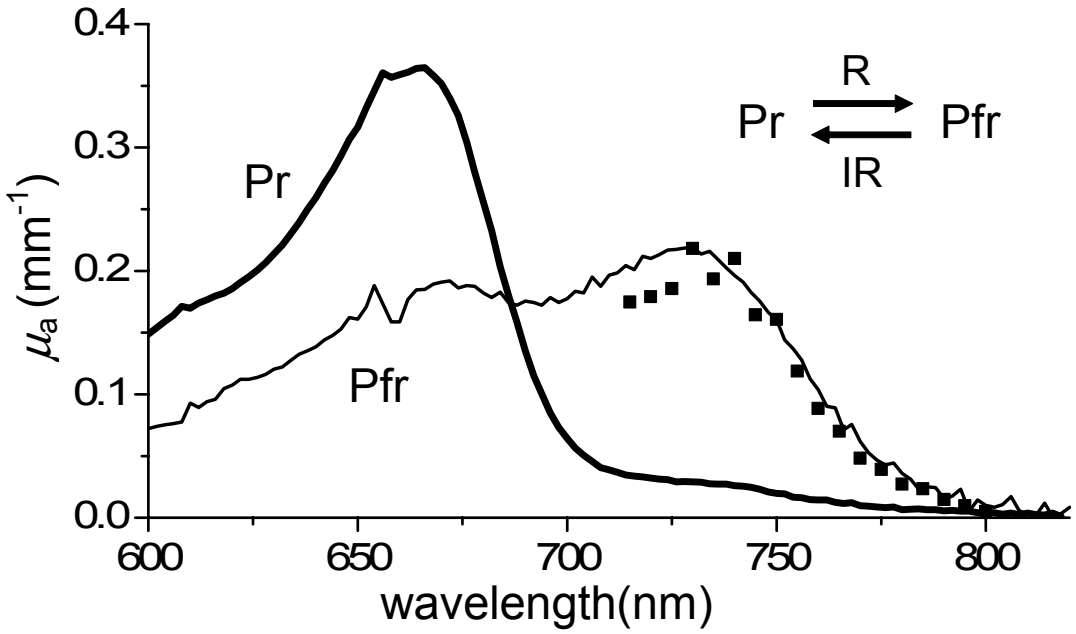

Figure 1: Absorption spectra of PhyA (conc. of 83 μM) in its Pr and Pfr state. The solid dots are the observed absorption coefficient change at different OCT probe (intensity ~10mW/cm^2) wavelengths when the molecules are forced from one state to the other by the pump light (intensity ~200mW/cm^2) of wavelength 660nm.

The protein that we have chosen to focus on is phytochrome A (phyA) [5]. This protein is expressed in all plants and serves as part of the photoperiodic mechanism for flowering, leafing, chloroplast development and germination. The molecular weight of the protein is about 120kDa. Each covalently bonds with a pigment molecule – tetrapyrrole. This protein can reversibly switch between two states with different absorption maxima upon illumination by light of suitable wavelengths. The spectrum shift is due to a conformational change in the protein structure during light activation. The two states of phytochrome are Pr and Pfr, respectively. The Pr form absorbs strongly at around 666nm. It is also the natural form that phyA is synthesized by dark-grown seedlings in and is the form that phyA reverts to in the absence of light. Upon absorption of red light, Pr converts into the Pfr form. The Pfr form absorbs strongly around 730nm. Biologically, this is the active form that initiates various biological responses in the plants. Upon absorption of near infrared red light, Pfr converts into the Pr form.

We begin our experiments with phyA by first characterizing the conditions for state switching and the relative absorption change. We then demonstrate a viable MCOCT scheme that can exploit the absorption change to profile phyA's distribution within a target sample. Finally, we show an experimental implementation of the method and demonstrate its capability in localizing the protein in a scattering medium. To our knowledge, this is the first demonstration of a molecular contrast OCT scheme that is capable of imaging the distribution of a protein based agent within a target sample.

We acquired phyA from Kumho Life & Environmental Science Laboratory. The protein is purified from dark grown oats. In its native state Pfr, phyA is experimentally verified to absorb strongly in the spectral range of 730nm (see

Fig. 1; the measurement is acquired from a 83 μM conc. sample on a HP8452A spectrophotometer). Upon illumination with light which wavelength falls within the absorption spectrum, phyA transits into its alternate state, Pr. With 750nm illumination at an intensity of 200mW/cm^2, the transit time is observed to be 140ms. The state Pr's absorption maximum is 660nm (see Fig. 1; the measurement is acquired from the same sample after the sample has been illuminated with 750nm light). It is observed that the protein will return to its native Pfr state within several seconds after the excitation light is removed. The return can be expedited by illuminating the sample with light which wavelength falls within the absorption spectrum of Pr. With 660nm illumination at an intensity of 200mW/cm^2, the return time is observed to be 170ms.

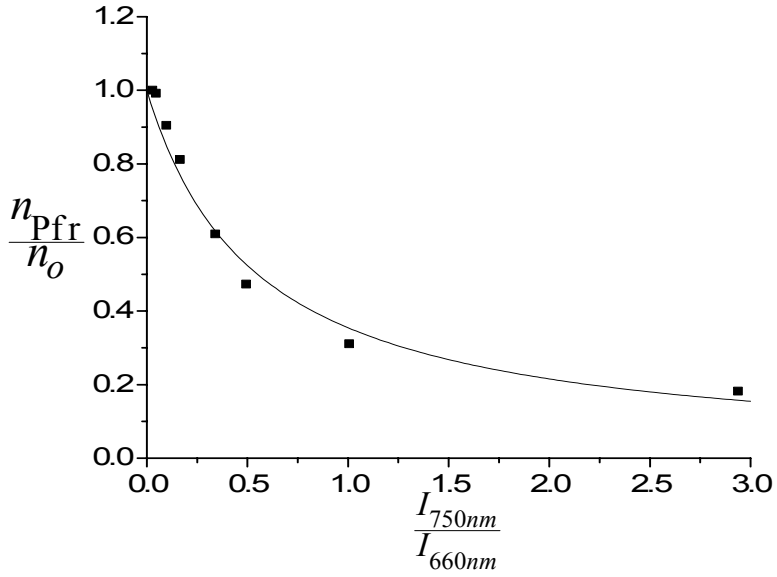

Figure 2: Plot of the observed fractional population undergoing state change versus the ratio of 750nm probe light to 660nm pump light used. The solid line is the best fit based on Eq. (2).

As OCT depth penetration is better at longer wavelengths, we choose our MCOCT probe wavelength to fall within the absorption spectrum of Pfr state. In the absence of other illumination source, the intensity of the OCT probe light (typically ~ 300 W/cm^2) is more than sufficient to cause phyA to transit into its Pr state. To force phyA into its Pfr state while the OCT probe light is on, we coilluminate the sample with a 660nm pump light at a high intensity. In other words, the MCOCT image acquisition scheme involves a constant illumination of the sample with the OCT probe light and alternately switching off and on the 660nm pump light to switch phyA between its Pr and Pfr state. The ratio of 660nm light intensity (I_{660nm}) to 750nm light intensity (I_{750nm}) required to cause a sufficient state change is governed by the rate equation:

$$\frac{dn_{\mathrm{Pfr}}}{dt} = -\frac{\sigma_{\mathrm{Pfr},750nm}\varepsilon_{IR}}{h\nu_{750nm}} I_{750nm} n_{\mathrm{Pfr}} + \frac{\sigma_{\mathrm{Pr},660nm}\varepsilon_{R}}{h\nu_{660nm}} I_{660nm}(n_o - n_{\mathrm{Pfr}}) + \frac{(n_o - n_{\mathrm{Pfr}})}{\tau_{\mathrm{Pr}}}, \qquad (1)$$

where n_o is the total PhyA conc., n_{Pfr} is the conc. of PhyA in Pfr state, $h\nu$ is the photon energy at the stated wavelength, $\sigma_{\mathrm{Pfr},750nm}$ ($\sigma_{\mathrm{Pr},660nm}$) is the absorption cross-section of Pfr (Pr) state at 750nm (660nm), τ_{Pr} is the natural decay time of Pr to Pfr state (this term is very weak and shall henceforth be ignored), ε_R and ε_{IR} is the quantum efficiency of the transition from Pr to Pfr and vice verse, respectively. Under steady state consideration, we get:

$$\frac{n_{\mathrm{Pfr}}}{n_o} \approx 1 \Big/ 1 + \frac{\nu_{660nm}\varepsilon_{IR}\sigma_{\mathrm{Pfr},750nm}}{\nu_{750nm}\varepsilon_{R}\sigma_{\mathrm{Pr},660nm}} \frac{I_{750nm}}{I_{660nm}} = \frac{1}{1 + a\dfrac{I_{750nm}}{I_{660nm}}}, \qquad (2)$$

where a represents the rate factor. We determine this factor to be (1.82 ± 0.18) by performing a set of transmission measurement experiment where the transmission of 750nm light, of intensity ranging from 10mW/cm^2 to 600mW/cm^2, through a 1cm cuvette filled with 83μM conc. of PhyA was measured while an illumination at 660nm of intensity 200mW/cm^2 was alternately switched on and off (see Fig. 2).

The wavelength choice of 750nm is arrived through a similar set of transmission experiment. In this set of experiment, the probe light intensity is kept constant and sufficiently low (~10mW/cm^2). The pump light (intensity ~200mW/cm^2) is then alternately switched on and off, the absorption change is measured and plotted in Fig 1. From the data, we can see that 730nm is the optimal probe wavelength at which maximal phyA absorption change occurs. As a compromise for deeper depth penetration in scattering medium, the wavelength of 750nm is selected for our application.

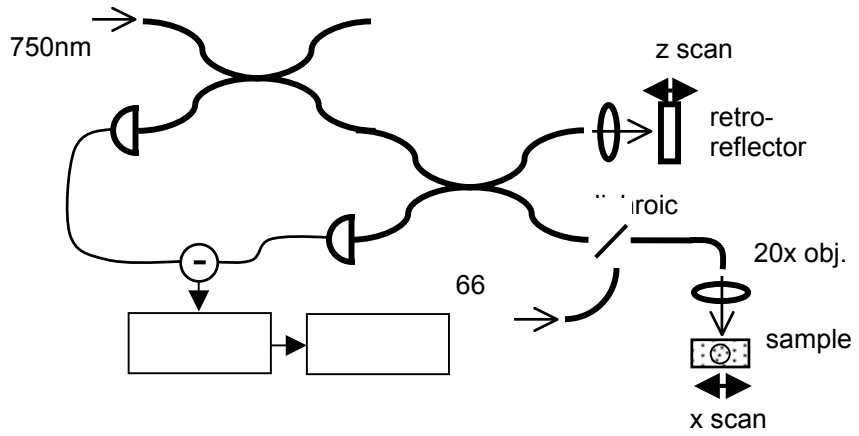

Figure 3: Experimental setup.

3. EXPERIMENT

The MCOCT experimental setup that we employed is depicted in Fig. 3. A tunable Spectra-Physics Tsunami Ti:Sapphire laser with FHWM linewidth of 11nm serves as our OCT probe light source and is coupled into the setup at point A. Part of the light (reference), P_{Ro}, is retroreflected at point B and recoupled back into the interferometer. The scanning galvo at point B creates a Doppler frequency upshift of 41kHz on the reflected reference beam. The remainder of the light, P_{So}, is combined with 660nm light from a Power Technology PPM20/6393 laser diode in a OZ Optics QSMF-488-3.5/125-0.5-L dichroic combiner. The combined beam is then focused (Newport M-20X objective) onto a target sample and the backscattered light (signal) is recoupled back into the interferometer. The FWHM of the focal spot on the sample is about 6.9 μm and the depth of focus is 124 μm. The typical 750nm and 660nm power incident on the sample is 104μW and 433μW, respectively. This ensures that we get a significant fraction of PhyA switching between Pr and Pfr state during the scans. The interfering signal and reference light is detected using an New Focus Model 2007 auto-balanced detector. A Stanford Research Systems SR830 lock-in amplifier processes the detected signal and outputs the amplitude of the heterodyne component into a National Instruments DAQCard-6062E ADC in a computer. The 660nm illumination is controlled through an OZ Optics TTL gated optical switch by the acquisition program running on the same computer. The system acquires 2mm optical path length a-scans at a rate of approximately 5Hz.

We note that the 750nm probe light is always kept on the sample during the entire imaging process. The image acquisition process involves the following steps: 1) the 660nm illumination is switched on, 2) after a pause of 500ms to

allow time for phyA to transit into its Pfr state, an averaged Pfr A-scan is obtained by acquiring and averaging over 300 A-scans, 3) the 660nm light is turned off, 4) after a pause of 500ms to allow phyA to switch into its Pr state, an averaged Pr A-scan is obtained by acquiring and averaging over 300 A-scans, 5) the sample is displaced laterally by a small increment and the process is repeated.

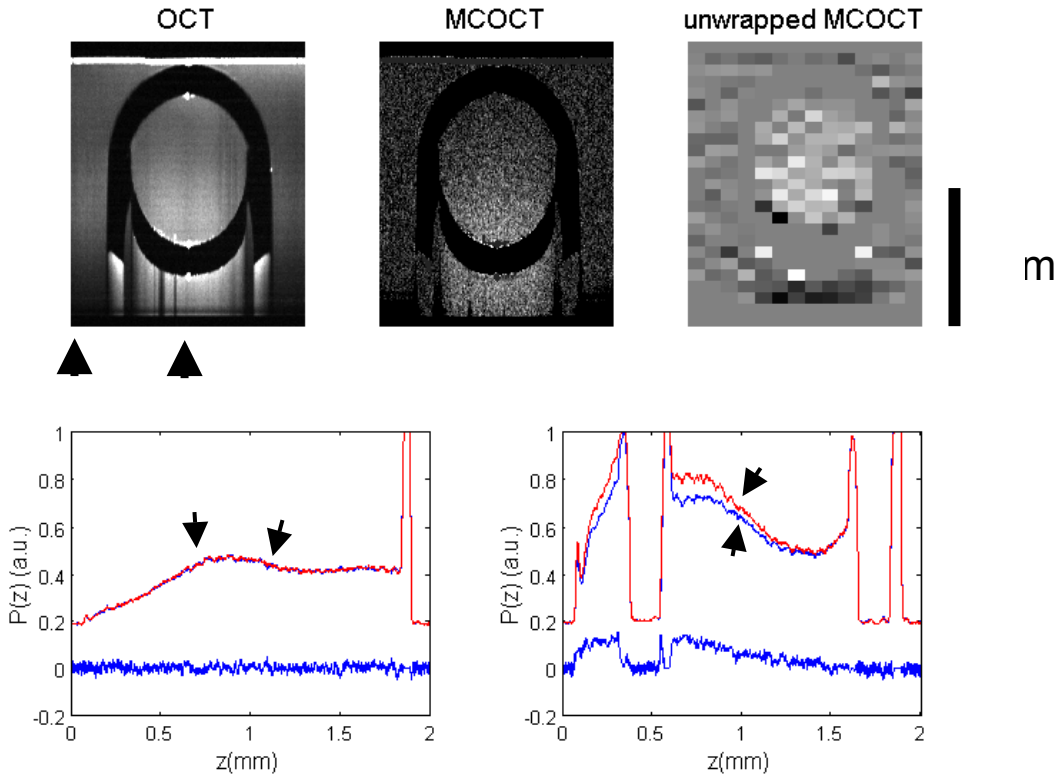

Figure 4: a) 750nm OCT b-scan with PhyA in Pr state(1.5mm × 2mm); the OCT b-scan (not shown) with PhyA in Pfr state appears very similar. b) MCOCT scan derived based on the operations described in Eq. (4). c) Unwrapped MCOCT scan derived based on the operations described in Eq. (5). d) A-scans with PhyA in Pr and Pfr state extracted from the location indicated in Fig. 1(a). The ratio trace is from a same location from Fig. 1(b). e) A-scans with PhyA in Pr and Pfr state extracted from the location indicated in Fig. 1(a). The ratio trace is from a same location from Fig. 1(b).

4. ANALYSIS

Figure 4(a) shows the resulting 300×4000 pixels B-scan created by compiling the averaged A-scans. The sample comprises of a 1mm thick capillary tube filled with 83 μM conc. of phyA in 0.2 % intralipid inserted into a 2mm cuvette filled with 0.2 % intralipid. Figure 4(d) and 4(e) shows the averaged Pfr and Pr A-scans along different positions of the sample. Not surprisingly, Pfr and Pr A-scans shows a difference only for the pair that are acquired across the PhyA containing capillary. The increasing difference at greater depth is due to the cumulative effect of absorption on the OCT signal. More explicitly, the OCT signal, $P(z)$, from a given depth z in the sample is given by:

$$P(z) = 2\sqrt{P_{So}P_{Ro}}\sqrt{R(z)}\exp\left(-\int_0^z \mu_a(z') + \mu_a(z')\,dz'\right), \qquad (3)$$

where $R(z)$ is the depth dependant collected back-scattered light from the sample (which includes effects due to focal parameters), $\mu_a(z)$ and $\mu_s(z)$ are the extinction and scattering coefficients at depth z, respectively. Between Pfr and Pr A-scans, $\mu_a(z)$ is changed significantly and its presence in the integration term of Eq. (3) leads to the cumulative increase in signal difference.

We can generate an MCOCT image that shows only this $\mu_a(z)$ by processing the Pfr, $P_{\mathrm{Pr}}(z)$, and Pr, $P_{\mathrm{Pfr}}(z)$, scans in the following manner:

$$\ln\left(\frac{P_{\mathrm{Pr}}(z)}{P_{\mathrm{Pfr}}(z)}\right) = \int_0^z \mu_{a,\mathrm{Pfr}}(z') - \mu_{a,\mathrm{Pr}}(z')\, dz' = \int_0^z \Delta\mu_a(z')\, dz' . \qquad (4)$$

Figure 4(b) shows the result of such a processing. The effect of the absorption change can be clearly seen and the presence of phyA within the capillary is evident. Figure 4(d) and 4(e) shows the processed A-scans along different positions of the sample.

The processed scans can be further processed and unwrapped to eliminate the integrative effect. Mathematically, the processing can be expressed as:

$$\ln\left(\frac{P_{\mathrm{Pr}}(z+\Delta z)}{P_{\mathrm{Pfr}}(z+\Delta z)}\right) - \ln\left(\frac{P_{\mathrm{Pr}}(z)}{P_{\mathrm{Pfr}}(z)}\right) = \int_z^{z+\Delta z} \Delta\mu_a(z')\, dz' \approx \Delta\mu_a(z)\Delta z \qquad (5)$$

Due to the derivative nature of this processing, it is highly susceptible to noise. Figure 4(c) shows the result where $\Delta z = 80\mu m$ is used and spatial averaging over 20 x 160 pixel is done. The heightened signal within the capillary indicates phyA's presence.

The use of phyA under these reported experimental conditions appears very appropriate. In a separate experiment to detect any photo-induced damage on phyA, we subjected the phytochrome to 1000 cycles of Pr → Pfr → Pr change. The amount of contrast change did not degrade to any observable extent through the entire experiment.

In addition to our demonstration of phyA as a viable MCOCT contrast agent, its candidacy as a potential protein based contrast agent is further supported by the capability of biologists to genetically manipulate its associated DNAs. To date, the transfection of phyA's DNA and the expression of phyA have been reported for yeast and E. coli [7]. PhyA can potentially fulfill the role of an endogenously expressed contrast agent for MCOCT, very much in the same manner that GFP is presently employed as an expressible protein contrast agent for fluorescence microscopy applications.

In conclusion, we demonstrated that PhyA, a plant derived protein, is a suitable contrast agent for MCOCT application. We are able to render depth resolved images that reveal PhyA's presence, at a conc. of 83 μM, within a sample at light intensity levels that are safe for in-vivo applications.

This research was supported by NIH grant no. EB000243. C Yang's email address is chyang@caltech.edu.

REFERENCES

1. Denk, W., J.H. Strickler, and W.W. Webb, *2-Photon Laser Scanning Fluorescence Microscopy.* Science, 1990. **248**(4951): p. 73-76.
2. Rao, K.D., et al., *Molecular contrast in optical coherence tomography by use of a pump-probe technique.* Optics Letters, 2003. **28**(5): p. 340-342.
3. Lee, T.M., et al., *Engineered microsphere contrast agents for optical coherence tomography.* Optics Letters, 2003. **28**(17): p. 1546-1548.
4. Kohler, R.H., et al., *The green fluorescent protein as a marker to visualize plant mitochondria in vivo.* Plant Journal, 1997. **11**(3): p. 613-621.
5. Fankhauser, C., *The phytochromes, a familiy of red/far-red absorbing photoreceptors.* Journal of Biological Chemistry, 2001. **276**: p. 11453-11456.
6. An, K.W., et al., *Cavity Ring-Down Technique and Its Application to the Measurement of Ultraslow Velocities.* Optics Letters, 1995. **20**(9): p. 1068-1070.
7. Gartner, W., et al., *Influence of expression system on chromophore binding and preservation of spectral properties in recombinant phytochrome A.* European Journal of Biochemistry, 1996. **236**: p. 978-983.